

## 10-(2-oxo-2-Phenylethylidene)-10H-anthracen-9-ones as Highly Active Antimicrotubule Agents: Synthesis, Antiproliferative Activity, and Inhibition of Tubulin Polymerization

Helge Prinz,<sup>\*,†</sup> Peter Schmidt,<sup>‡</sup> Konrad J. Böhm,<sup>§</sup> Silke Baasner,<sup>‡</sup> Klaus Müller,<sup>†</sup> Eberhard Unger,<sup>§</sup> Matthias Gerlach,<sup>‡</sup> and Eckhard G. Günther<sup>‡</sup>

*Institute of Pharmaceutical and Medicinal Chemistry, Westphalian Wilhelms-University, Hittorfstrasse 58-62, D-48149 Münster, Germany, Leibniz Institute for Age Research—Fritz Lipmann Institute (FLI), Beutenbergstrasse 11, D-07745 Jena, Germany, AeternaZentaris GmbH, Weismüllerstrasse 50, D-60314 Frankfurt, Germany*

Received October 23, 2008

A series of 10-(2-oxo-2-phenylethylidene)-10H-anthracen-9-ones were synthesized and evaluated for interactions with tubulin and for antiproliferative activity against a panel of human and rodent tumor cell lines. The 4-methoxy analogue **17b** was most potent, displaying IC<sub>50</sub> values ranging from 40 to 80 nM, including multidrug resistant phenotypes, and had excellent activity as an inhibitor of tubulin polymerization (IC<sub>50</sub> = 0.52 μM). Concentration-dependent flow cytometric studies showed that KB/HeLa cells treated with **17b** were arrested in the G2/M phases of the cell cycle (EC<sub>50</sub> = 90 nM). In competition experiments, **17b** strongly displaced [<sup>3</sup>H]-colchicine from its binding site in the tubulin. The results obtained demonstrate that the antiproliferative activity is related to the inhibition of tubulin polymerization.

### Introduction

The mitotic spindle, constituted by microtubules generated by polymerization of αβ-tubulin dimers, is considered one of the most important targets to treat many types of malignancies.<sup>1,2</sup> A still expanding family of antimitotic drugs displaying a wide structural heterogeneity have been identified to act on tubulin. Many of these agents work by inhibiting polymerization of tubulin into microtubules, others by stabilizing the microtubule structure.<sup>3–6</sup> The Vinca bis-indole alkaloids vinblastine (**1a**, Chart 1) and vincristine (**1b**) as well as the taxanes are well established to treat a broad range of leukemias and lymphomas as well as many types of solid tumors. It was mainly the discovery of these compounds that has stimulated intense efforts aimed at the development of further microtubule-targeting drugs. Colchicine (**2**) has not been successfully used as an anticancer agent, due primarily to its narrow therapeutic window, but played an important role in deciphering the properties and functions of tubulin and microtubules. Many natural products, such as combretastatin A-4<sup>7</sup> (**3**) or the epothilones<sup>8</sup> as well as some synthetic molecules including sulfonamide E-7010<sup>9</sup> (**4**), 4-anilinoquinazoline<sup>10</sup> (**5**), acridinyl-9-carboxamide D-82318<sup>11</sup> (**6**), indazole-based TH-482<sup>12</sup> (**7**), or propenenitrile CC-5079<sup>13</sup> (**8**) (Chart 1), to name just a few, are known to mediate antiproliferating activities through binding to tubulin. In recent years, substantial progress has been made in the identification of small-molecular colchicine-site binders derived from natural sources or by screening compound libraries in combination with traditional medicinal chemistry.<sup>3,5,14</sup> However, no representative of this class has yet been introduced into cancer chemotherapy.

We have recently reported the potent in vitro antitumor activity of 10-[(3-hydroxy-4-methoxy-benzylidene)]-9(10H)-anthracenone (**9**), 9-[(4-hydroxy-3,5-dimethoxy-benzylidene)-naphtho[2,3-*b*]thiophen-4(9H)-one (**10**) and 4-methoxybenze-

nesulfonic acid esters **11** and **12** (Chart 2).<sup>15–17</sup> These compounds strongly inhibited tumor cell growth, tubulin polymerization, and caused also significant arrest of mitosis. This previous work prompted us to extend our studies to structurally related anthracenone-based enone systems in which the anthracenone moiety is linked directly to the termini of an enone group. Several previous investigations on benzophenones, chalcones, and related enones have demonstrated their potent antimitotic activities.<sup>18,19</sup> In this report, we describe the synthesis and biological evaluation of 10-(2-oxo-2-phenylethylidene)-10H-anthracen-9-ones as novel tubulin polymerization inhibitors. Several of these compounds inhibited the growth of various tumor cell lines, acted in a cell-cycle-dependent manner, and were found to be potent inhibitors of tubulin polymerization. Antitubulin activity of the most active compound is comparable or superior to those of the reference compounds, such as nocodazole, podophyllotoxin, and colchicine.

### Chemistry

The general method for the synthesis of the novel 10-substituted anthracenones is outlined in Scheme 1. For the synthesis of compounds **17b**, **17d**, **17f**, **17g**, and **17j** as well as for **17l** and **17m**, the acid chloride **16** was synthesized from **13** and then reacted with suitable aromatic compounds in a Friedel–Crafts acylation reaction (Scheme 1). A drawback is that the reaction is limited to reactive arenes and therefore lacks variability. Therefore, the aldol condensation reaction of **13** with phenylglyoxal hydrates was thought to be an alternative method.<sup>20</sup> However, the synthesis of the desired 10-(2-oxo-2-phenylethylidene)-10H-anthracen-9-ones required a careful choice of the reaction conditions. Condensation reaction of 10H-anthracen-9-one **13** with aromatic aldehydes is generally applicable<sup>21</sup> and was thought to be the method of choice. Initial attempts using gaseous hydrogen chloride<sup>22,23</sup> or pyridine/piperidine<sup>24</sup> for the condensation reaction unexpectedly failed. For this reason, we investigated different reaction conditions. Performing the aldol-type reaction in ethanol/piperidine as described for **14**, afforded 10-(1-hydroxy-2-oxo-2-phenyl-ethyl)-10H-anthracen-9-ones **19a–c** (Scheme 2). Although these compounds proved to be ineffective in the biological assays

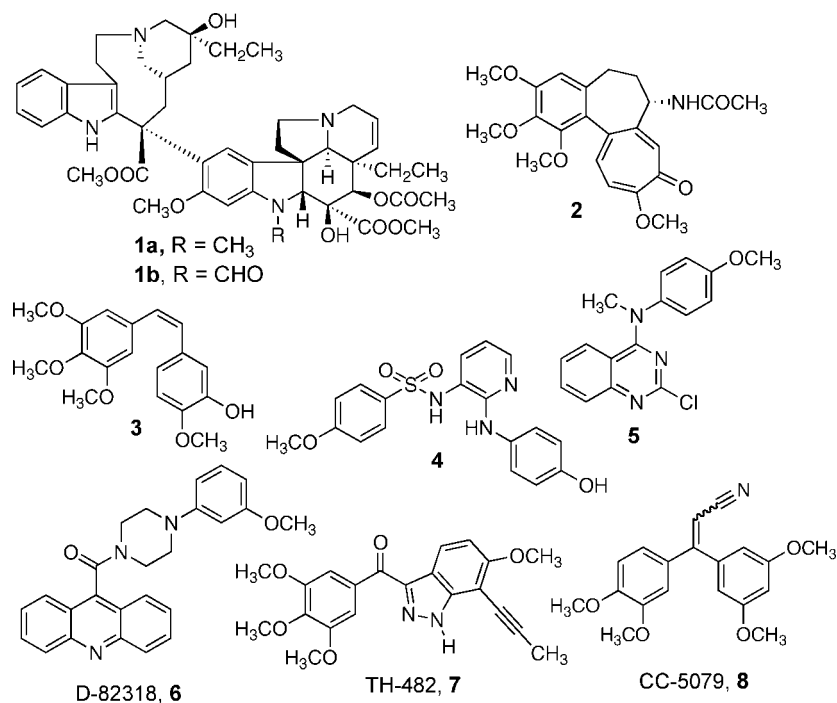
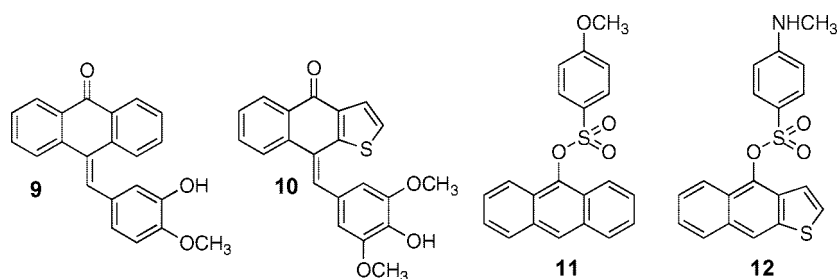
\* To whom correspondence should be addressed. Phone: +49 251-8332195. Fax: +49 251-8332144. E-mail: prinzh@uni-muenster.de.

<sup>†</sup> Institute of Pharmaceutical and Medicinal Chemistry, Westphalian Wilhelms-University.

<sup>‡</sup> AeternaZentaris.

<sup>§</sup> Leibniz Institute for Age Research—Fritz Lipmann Institute.

Chart 1. Examples of Tubulin Interacting Agents

Chart 2. Tubulin Interacting Benzylidenes **9** and **10** and Sulfonates **11** and **12**

(see below), they were valuable intermediates for further syntheses. In this connection, we additionally obtained **23** when **13** reacted with the aliphatic glyoxyl dimethylacetal under the same conditions. This is remarkable, as **13** is known to react only with more reactive aliphatic aldehydes. At the end, synthesis of further 10-(2-oxo-2-phenylethylidene)-10H-anthracen-9-ones (**17a**, **17c**, **17h**) was successfully accomplished by condensation reaction of **13** with appropriately substituted phenylglyoxal hydrates<sup>20</sup> in boiling acetic acid anhydride. The starting phenylglyoxal hydrates were obtained from commercial sources. For the preparation of compounds **17e**, **17i**, and **17k** (Scheme 1), ether groups of **17b**, **17d**, and **17g** had to be cleaved by BBr<sub>3</sub> in dichloromethane or AlCl<sub>3</sub> in DCE. As an important aspect, the use of phenylglyoxal derivatives enhanced the structural variability and especially gave access to constitutional isomers, which we suggested would not easily be obtained by means of Friedel–Crafts acylation reaction (**17b** versus **17c**, **17g** versus **17h**). For SAR studies and in order to investigate the relevance of the enone C=C-double bond, we were interested in the synthesis of **21**. However, attempts to alkylate<sup>15,25</sup> **13** at C-10 were unsuccessful (Scheme 3). Interestingly, in contrast to the previously described C-10 alkylation of 9(10H)anthracenone,<sup>15</sup> reaction of **13** with  $\alpha$ -bromoacetophenone in the presence of potassium carbonate in acetone afforded *O*-alkylated enol **22** instead of C-alkylation. Keto–enol tautomerism in the anthrone series has been described,<sup>26</sup> and the formation of

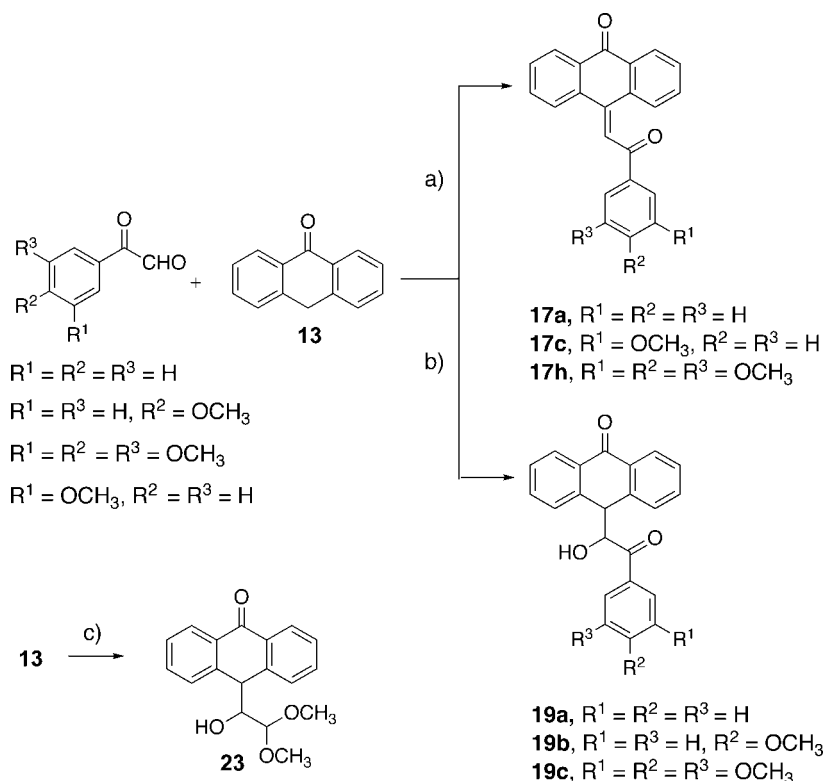
compound **22** is suggested to be due to a base-catalyzed enolization of **13**. Furthermore, to investigate the relevance of the anthracenone ketone function for activity, **17b** was selectively reduced using sodium borohydride to afford 10-hydroxy-substituted anthracenylidene **20** (Scheme 4). Esters **18a** and **18b** were initially prepared under conditions of the Friedel–Crafts acylation reaction as starting materials for the synthesis of hydroxy-methoxy aryl ketones. Unfortunately, preparation via Fries rearrangement reaction<sup>27</sup> of the esters by catalysis of Lewis acids failed.

## Biological Results and Discussion

**In Vitro Cell Growth Inhibition Assay.** In an initial screen, the compounds synthesized were evaluated for antiproliferative activity against the human chronic myelogenous leukemia cell line K562,<sup>28</sup> which is widely used for potential antitumor compounds. Cell proliferation was determined directly by counting the cells with a hemocytometer after 48 h of treatment. Table 1 summarizes the biological data for inhibition of K562 cell growth and inhibition of tubulin polymerization (see below). Data obtained with several reference compounds are also presented. In the 10-(2-oxo-2-phenylethylidene)-10H-anthracen-9-one series, five compounds (**17b**, **17e**, **17h**, **17j**, and **17l**) showed IC<sub>50</sub> values in the submicromolar (lower than 1  $\mu$ M) range. Compound **17b** was the most potent and displayed strong antiproliferative activity with an IC<sub>50</sub> value of lower than

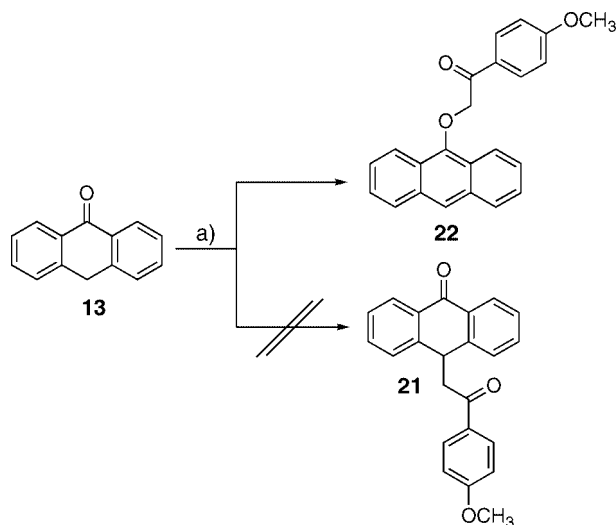


**Scheme 2.** R<sup>1</sup>–R<sup>3</sup> are defined in Table 1<sup>a</sup>



<sup>a</sup> Reagents and conditions: (a) 3-methoxyphenyl-, 3,4,5-trimethoxyphenyl-, or phenylglyoxal hydrate, (CH<sub>3</sub>CO)<sub>2</sub>O, reflux; (b) 3-methoxyphenyl-, 3,4,5-trimethoxyphenyl-, or phenylglyoxal hydrate, C<sub>2</sub>H<sub>5</sub>OH, piperidine, reflux, 6 h; (c) glyoxal dimethyl acetal (60% aq soln), C<sub>2</sub>H<sub>5</sub>OH, piperidine, reflux, 6 h.

**Scheme 3<sup>a</sup>**

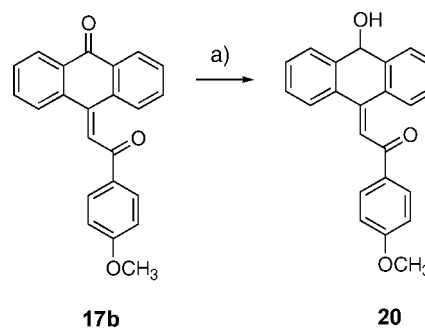


<sup>a</sup> Reagents and conditions: (a) 2-bromo-4'-methoxyacetophenone, K<sub>2</sub>CO<sub>3</sub>, acetone, reflux.

compared to **17b**. This finding demonstrated the importance of the intact anthracenone carbonyl functional group for potency. Also, 10-hydroxy-substituted anthracenylidene derivative **20** was among the most potent compounds, which gave rise to further derivatization within this series. However, partial oxidation of **20** under the conditions of the cellular assay can not be excluded at that point in time.

**Effect on Growth of Different Tumor Cell Lines.** To further characterize the tumor cell growth inhibitory profile of the compounds, the effect of the highly active *p*-methoxy analogue **17b** and analogues **17d** and **17e** against a panel of five tumor

**Scheme 4<sup>a</sup>**



<sup>a</sup> Reagents and conditions: (a) NaBH<sub>4</sub>, ethanol/THF, rt.

cell lines derived from human tumors was measured by cellular metabolic activity using the XTT<sup>a</sup> assay.<sup>29</sup> Of the tested compounds, **17b** displayed high overall potencies, with IC<sub>50</sub> values in the range of 60–80 nM toward several proliferating cell lines (Table 2). Thus **17b** showed activities comparable to those of colchicine. Compound **17e** was also confirmed to be active with IC<sub>50</sub> values ranging from 0.16 to 0.43 μM. Even **17d** was found to be effective, although potency was found to be substantially reduced. Furthermore, compounds **17b**, **17d**, and **17e** were not active against cell cycle arrested RKO cells (human colon adenocarcinoma) with ectopic inducible expression of cyclin-dependent kinase inhibitor p27<sup>kip1</sup>.<sup>30</sup> By contrast, growth of proliferating RKO<sub>p27</sub>-cells (not induced) was strongly

<sup>a</sup> Abbreviations: aq, aqueous; ADR, doxorubicin; CSI, colchicine site inhibitor; DCE, 1,2-dichloroethane; ITP, inhibition of tubulin polymerization; Kip, kinase inhibitor protein; MDR, multidrug resistant; MRP, multidrug resistance protein; MTP, microtubule protein; ND, not determined; soln, solution; VCR, vincristine; XTT, 2,3-bis-(2-methoxy-4-nitro-5-sulphophenyl)-2*H*-tetrazolium-5-carboxanilide.

**Table 1.** Inhibitory Effect of 10-(2-oxo-2-Phenylethylidene)-10H-anthracen-9-ones and Related Compounds on the Growth of K562 Cells and Tubulin Polymerization

compd	17a-k		17l, 17m	18a, 18b		19a-c	
	R <sup>1</sup>	R <sup>2</sup>	R <sup>3</sup>	R <sup>4</sup>	R <sup>5</sup>	K562 IC <sub>50</sub> <sup>a</sup> [μM]	ITP <sup>b</sup> IC <sub>50</sub> [μM]
15						6.0	ND
17a	H	H	H	H	H	3.60	5.0
17b	H	H	OCH <sub>3</sub>	H	H	0.07	0.52
17c	H	OCH <sub>3</sub>	H	H	H	2.60	3.3
17d	H	OCH <sub>3</sub>	OCH <sub>3</sub>	H	H	1.30	6
17e	H	OH	OH	H	H	0.16	2.6
17f	OCH <sub>3</sub>	H	OCH <sub>3</sub>	H	H	ND	0.9
17g	OCH <sub>3</sub>	OCH <sub>3</sub>	OCH <sub>3</sub>	H	H	11	>10
17h	H	OCH <sub>3</sub>	OCH <sub>3</sub>	OCH <sub>3</sub>	H	0.70	3.7
17i	OH	OCH <sub>3</sub>	OCH <sub>3</sub>	H	H	>30	>10
17j	H	H	CH <sub>3</sub>	H	H	0.64	1.1
17k	H	H	OH	H	H	3.43	0.9
17l	OCH <sub>3</sub>					0.69	2.3
17m	H					5.21	10
18a	OCH <sub>3</sub>	H	H	H	H	1.9	10
18b	OCH <sub>3</sub>	H	H	H	OCH <sub>3</sub>	1.64	10
19a	H	H	H			27	>10
19b	H	OCH <sub>3</sub>	H			18	>10
19c	OCH <sub>3</sub>	OCH <sub>3</sub>	OCH <sub>3</sub>			21	>10
20						0.21	1.20
22						10	ND
colchicine						0.02	1.4
nocodazole						ND	0.76
podophyllotoxin						ND	0.35
vinblastine sulfate						0.001	0.13
adriamycin						0.01	ND

<sup>a</sup> IC<sub>50</sub> values are the means of at least three independent determinations (SD < 10%). <sup>b</sup> ITP = inhibition of tubulin polymerization; IC<sub>50</sub> values were determined after 30 min at 37 °C and represent the concentration for 50% inhibition of the maximum tubulin assembly rate.

**Table 2.** Antiproliferative Activity of **17b**, **17d**, and **17e** against Different Tumor Cell Lines<sup>a</sup>

compd	IC <sub>50</sub> <sup>a</sup> [μM]					RKOp27 <sup>kip</sup>	
	KB/HeLa	SKOV3	SF268	NCI-H460	not induced		
					induced	induced	
17b	0.06	0.06	0.06	0.07	0.08	>9	
17d	1.08	ND	2.7	1.4	0.51	>9	
17e	0.27	0.16	0.22	0.43	0.24	>9	
paclitaxel	0.01	0.01	0.01	0.01	0.01	>3	
nocodazole	0.14	0.17	0.30	0.15	0.11	>10	
colchicine	0.03	0.05	0.05	0.07	0.02	>10	

<sup>a</sup> All experiments were performed at least in two replicates ( $n = 2$ ), and IC<sub>50</sub> data were calculated from dose–response curves by nonlinear regression analysis.

inhibited by **17b**, with an IC<sub>50</sub> value of 0.08 μM and, somewhat less potent, by **17e** (IC<sub>50</sub> = 0.24 μM) and **17d** (IC<sub>50</sub> = 0.51 μM), indicating activity in cells, which were not arrested in G<sub>1</sub>-phase. Tubulin-targeting agents are used extensively for the treatment of many human malignancies, leading frequently to multiple drug resistance (MDR) in patients and a loss of efficacy over time. As a major problem, cancer cells do not respond to treatment or develop a broad spectrum resistance to several anticancer drugs, among them antitubulin agents.<sup>31,32</sup> Multiple drug resistance is multifaceted phenomenon and mediated, among other factors, by overexpression of transmembrane

**Table 3.** Antiproliferative Activity of **17b** and **17d**, Paclitaxel, Nocodazole, and Vindesine against Tumor Cell Lines with Different Resistance Phenotypes (XTT Assay)<sup>a</sup>

	IC <sub>50</sub> <sup>a</sup> [μM]						
	LT12	LT12 MDR	L1210	L1210 VCR	P388	P388 ADR	
17b	0.05	0.05	0.05	0.05	0.04	0.05	
17d	0.37	0.44	0.97	0.97	0.90	1.1	
paclitaxel	0.006	0.40	0.06	>5	0.04	>5	
nocodazole	0.30	0.05	0.06	0.07	0.07	0.05	
vindesine	0.001	0.26	0.02	>5	0.01	1.10	

<sup>a</sup> All experiments were performed at least in two replicates ( $n = 2$ ), and IC<sub>50</sub> data were calculated from dose–response curves by nonlinear regression analysis.

cellular pumps, such as the 170 kDa P-glycoprotein (P-gp),<sup>33</sup> encoded by the *mdr1* gene and the 180 kDa MDR protein (MRP).<sup>34</sup> Important aspects concerning the key mechanisms of antimicrotubule drug resistance have recently been reviewed.<sup>31,35,36</sup> Because colchicine, nocodazole, and paclitaxel are substrates for the P-gp efflux pump, we compared them with representative compounds **17b** and **17d** on the proliferation of tumor cell lines with different resistance phenotypes in an XTT-based assay. On the whole, as documented by the IC<sub>50</sub> data (Table 3), **17b** and even **17d** were effective against the wild type cell lines and retained high activity in cell lines with various MDR phenotypes. This behavior was distinct from reference compounds like paclitaxel and vindesine, which expressed only low

**Table 4.** Cell Cycle Analysis of KB/HeLa Cells Treated with **17b** and Reference Compounds Vincristine, Colchicine, Paclitaxel, and nocodazole

	<b>17b</b>	colchicine	nocodazole	paclitaxel	vincristine
EC <sub>50</sub> <sup>a</sup> [nM]	90	14	91	49	2.4

<sup>a</sup> EC<sub>50</sub> values were determined from dose–response cell cycle analysis experiments and represent the concentration for 50% cells arrested in G2/M phase after 24 h. All experiments were performed at least in two replicates ( $n = 2$ ), and EC<sub>50</sub> data were calculated from dose–response curves by nonlinear regression analysis (GraphPad Prism).

activity in LT12MDR, L1210VCR, and P388ADR cell lines (IC<sub>50</sub> data ranging from 0.26 to >5 μM) than to the wild type cell lines. We therefore conclude that the 10-(2-oxo-2-phenylethylidene)-10H-anthracen-9-ones investigated here are not substrates of the P-gp efflux pump. However, the effect of selective pressure of **17b** on the nonresistant cell lines eventually leading to an MDR status has not been studied yet.

**Effect on Cell-Cycle Progression.** By targeting the mitotic spindle, microtubule inhibitors arrest the cell cycle during the metaphase phase. As a consequence, mitosis is blocked at the transition from metaphase to anaphase. To gain further insight into the mode of action, the most active compound **17b** was assayed for its effects on cell cycle using an established KB/HeLa (human cervical epitheloid carcinoma) cell-based assay system. For a thorough comparison of **17b** with known G2/M cell cycle inhibitors, subconfluent KB/HeLa cells were exposed to test compounds and the percentage of cells in G2/M phase after 24 h was plotted against different concentrations of the compounds. The concentration for 50% cells arrested in G2/M phase by **17b** was found to be in the range of 90 nM (Table 4), thus being as active as nocodazole (EC<sub>50</sub> = 91 nM). For comparison, the recently described anthracenone derivative **9** showed an EC<sub>50</sub> value of 0.2 μM in a contemporaneous experiment. In summary, the effect of **17b** on cell cycle progression correlated well with its strong antiproliferative and antitubulin activity and is similar to that observed for the majority of antimetabolic agents. However, in this assay, the reference compounds were comparable or superior to **17b**, with the order of activity vincristine > colchicine > paclitaxel > nocodazole ~ **17b**.

**In Vitro Tubulin Polymerization Assays.** To investigate whether the antiproliferative activities of the novel compounds were related to an interaction with tubulin, 21 analogues were assayed for their inhibitory effects on tubulin polymerization using assay conditions as described previously.<sup>16</sup> If an inhibitor binds to or interferes with tubulin, the assembly steady-state level is decreased, as exemplified for **17b** (Figure 1). The results obtained with the test agents are summarized in Table 1. For comparison, the potent antimetabolic compounds colchicine, podophyllotoxin, nocodazole, and vinblastine were also examined. Compound **17b** was again the most potent (ITP; IC<sub>50</sub> = 0.52 μM), having nearly twice the potency of **17f** (ITP; IC<sub>50</sub> = 0.9 μM), **17j** (ITP; IC<sub>50</sub> = 1.1 μM), and **17k** (ITP; IC<sub>50</sub> = 0.9 μM). Nevertheless, these four compounds proved to be exceptionally strong inhibitors of tubulin polymerization (IC<sub>50</sub> ≤ 1.1 μM), as did the reference drugs with the exception of colchicine (ITP; IC<sub>50</sub> = 1.4 μM). Seven other compounds had IC<sub>50</sub> values ranging from 1.2–6 μM and were relatively potent tubulin polymerization inhibitors. In general, compounds having IC<sub>50</sub> values in the range of ≥10 μM were regarded to have no appreciable activity as an inhibitor of tubulin polymerization. Obviously, there is more variability in the IC<sub>50</sub> data for inhibition of K562 cell growth (Table 1) than in the IC<sub>50</sub> values for inhibition of tubulin polymerization. For example, we found

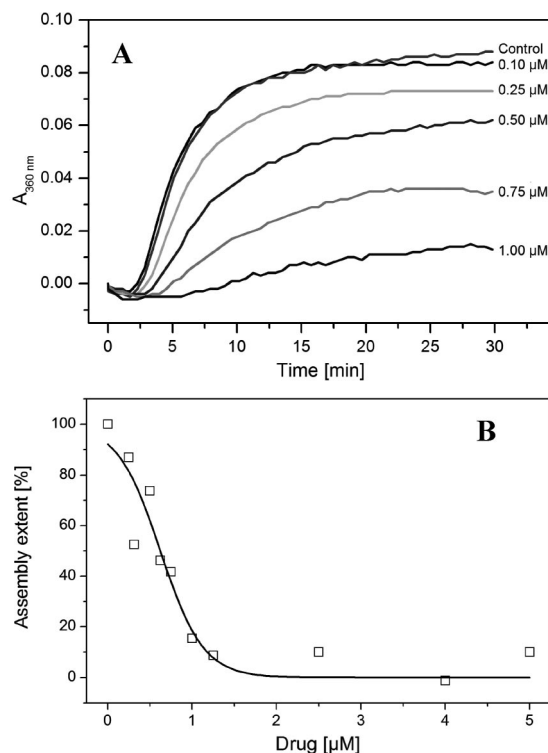


**Figure 1.** (A) Inhibition of in vitro polymerization of tubulin (in total 1.2 mg/mL protein; ~85% tubulin plus ~15% microtubule-associated proteins) at 37 °C by various concentrations of **17b** (IC<sub>50</sub> = 0.52 μM). The steady-state tubulin assembly level in the absence of inhibitor was set 100%. (B) IC<sub>50</sub> values were determined by sigmoidal fitting the plot of the steady state levels of tubulin assembly (taken 30 min after the temperature had been switched from 0 to 37 °C) against drug concentration and represent the concentration for 50% inhibition of the maximum tubulin polymerization level.

**17b** to be 2.1-fold more potent than **17j** as a tubulin polymerization inhibitor but found it to be 9.1 times more potent than **17j** in the growth inhibitory assay. This is probably due to the fact that the tumor cell growth assay and the cell-free tubulin polymerization assay differ in a number of important issues, such as tubulin concentration present within the cells, the presence of different types of microtubule-associated proteins as well as the possible effects of regulatory proteins expressed in the cell but being absent in the tubulin assay. Another aspect could be differences in cell permeability of the various compounds. Moreover, compound **20** (ITP; IC<sub>50</sub> = 1.20 μM) was slightly more potent than colchicine. Similar to the cell growth inhibition assay, this documented that tubulin polymerization inhibiting properties can also be found with 10-hydroxy-substituted anthracenylidenes as exemplified by **20**. The moderate to weak inhibitors of tumor cell growth showed only poor inhibitory effects on tubulin polymerization.

Microtubule-destabilizing drugs often reveal specific tubulin binding sites. Therefore, we determined if **17b** interacted directly with tubulin by binding to either the colchicine or paclitaxel-binding domains on tubulin using a competition-binding scintillation proximity assay.<sup>37</sup> We found that **17b** inhibited [<sup>3</sup>H]colchicine binding to biotinylated tubulin (Figure 2) with an IC<sub>50</sub> value of 0.40 μM versus colchicine (IC<sub>50</sub> = 1.06 μM). This result was consistent with the growth inhibitory and tubulin polymerization inhibitory activity. However, **17b** did not compete with [<sup>3</sup>H]paclitaxel (IC<sub>50</sub> > 100 μM). No stabilization of the colchicine binding was observed, as it is documented for Vinca site binders.<sup>38,39</sup> Therefore, we conclude that binding to tubulin at the colchicine-binding site is likely and that the

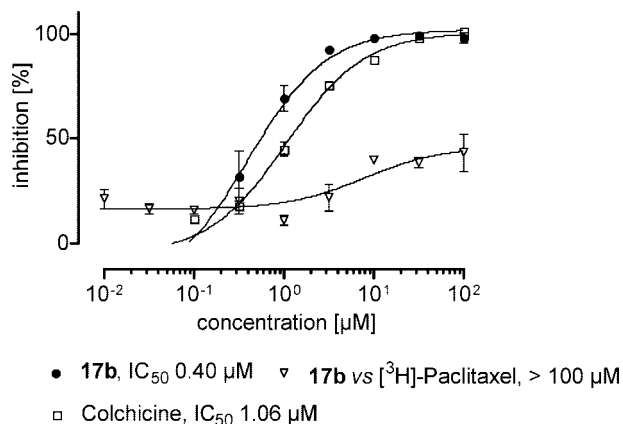


**Figure 2.** [<sup>3</sup>H] Colchicine competition binding assay of **17b** and colchicine. Radiolabeled colchicine or paclitaxel, unlabeled compound, and biotin-labeled tubulin were incubated together for 2 h at 37 °C.

capacity to interact with the mitotic spindle contributes to the antiproliferative activity of **17b**. A large number of synthetic and natural compounds with diverse structures have been shown to bind at the colchicine site, one of the major binding sites on tubulin, and to inhibit tubulin assembly. The diffraction map of a close structural analogue of colchicine bound to  $\alpha\beta$ -tubulin was reported in 2004.<sup>40</sup> On the basis of these important findings, computer simulation models have recently been employed to explain empirical structure–activity relationships of colchicine site inhibitors (CSIs) of tubulin polymerization.<sup>41,42</sup> The most active analogue **17b** contains some potential pharmacophore fragments such as the oxygen atom of the anthracenone carbonyl group as well as the oxygen atom and the methyl group of the methoxy substituent. In terms of the common pharmacophore<sup>41</sup> and consistent with our experimental data, the methoxy group in **17b** as well as the -hydroxy/-methoxy groups in **9**, **10** (Chart 2) are substituents of choice in the terminal aryl ring and are critical for activity. As seen with several other CSIs,<sup>41</sup> the carbon atom of the methoxy group in **17b** might probably function as a hydrophobic center. Both the methoxy group and the terminal aryl ring are essential features for activity.<sup>41,42</sup> A phenolic hydroxy group being flanked by one or two methoxy groups (**9**, **10**, Chart 2) is another important determinant for activity within the anthracenone derived CSIs,<sup>15,16</sup> with the hydroxy group possibly hydrogen-bonding to a suitable tubulin residue in the binding site. It has recently been hypothesized that the terminal isovanillinyl ring in **9** possibly binds to the same region of the protein as the pseudoaromatic tropone ring C in colchicine.<sup>42</sup> Interestingly, as documented by our earlier work, the isovanillinyl partial structure could not be successfully replaced by trimethoxy (a prominent pharmacophore present in many CSIs) with retention of high activity. A similar observation has been made with trimethoxy analogue **17h**, displaying an approximately 7-fold drop in potency in comparison with **17b** for the inhibition of tubulin polymerization. According to the published data,<sup>41</sup> the trimethoxyphenyl ring in colchicine, podophyllotoxin, CA-4, and steganacin constitutes an important hydrophobic center. It has been demonstrated by X-ray diffraction studies that the trimethoxyphenyl groups for a close colchicine analogue and for podophyllotoxin are located in the  $\beta$ -tubulin structure near the amino acid residue Cys239.<sup>40</sup> On the basis of our data, the significantly larger hydrophobic trimethoxy moiety in **17h** relative to the methoxy in **17b** is in general not well tolerated in the terminal aryl ring in the anthracenone based CSIs. On condition that the terminal isovanillinyl ring in **9**, and thus the methoxy-substituted ring

in **17b**, bind to the same region as the colchicine C ring,<sup>42</sup> we hypothesize that the anthracenone system might function as a hydrophobic center, similar to the colchicine A ring. The anthracenone carbonyl oxygen probably has importance as a hydrogen bond acceptor. Reduction of this carbonyl group resulted in a decreased inhibition of tubulin polymerization. The novel compounds **17a–17m** embody an enone group as a linker between two aryl groups. The carbonyl function in the linker between the terminal aryl ring and the anthracenone part might provide additional binding features. Obviously, this carbonyl group in **17b** could be accommodated by the colchicine binding site, which is supported by very similar data obtained from the [<sup>3</sup>H]colchicine binding assay for both **17b** and **9** (**9**, 0.37 μM; **17b**, 0.40 μM). However, it has to be pointed out that this structural modification gave no substantially greater potency of **17b** relative to **9** for the inhibition of tubulin polymerization (**9**, 0.67 μM; **17b** 0.52 μM). Notably, while the tubulin activities differ only slightly, we found **17b** to be 3.5-fold less active than **9** as an inhibitor of K562 tumor cell growth. We found, that the C=C double-bond linking the anthracenone system and the terminal aryl ring is also critical for activity. Saturation and hydroxylation of the alkene (**19a–c**) resulted in a significant loss of activity, indicating the importance of a more restricted conformational flexibility in the linker region. This is also confirmed by strongly decreased activities for C-10-benzylated analogues of **9**, as documented in our earlier work.<sup>15</sup>

## Conclusion

As an extension of our previously published work, we have presented synthetic inhibitors of tubulin polymerization based on a 10-(2-oxo-2-phenylethylidene)-10H-anthracen-9-one molecular skeleton with **17b** being a novel and potent antimetabolic agent. Similar to many other inhibitors of tubulin polymerization, selected compounds were efficacious in inhibiting tumor cell proliferation with IC<sub>50</sub> values at the submicromolar level. The best results for inhibition of antiproliferative activity were obtained with the *para*-methoxy derivative **17b**. In accordance with our previous findings, the 4-methoxy substitution pattern in the terminal phenyl ring is again critical for both strong inhibition of tumor cell proliferation and inhibition of tubulin polymerization. It is obvious that one of the molecular targets of the investigated compounds is the tubulin system. Compound **17b** is an excellent inhibitor of tubulin polymerization and most likely interacts with tubulin at the colchicine site. However, with the insertion of an additional carbonyl group in the linker, we obtained no substantially greater potency of **17b** relative to the recently described, structurally related **9** for the inhibition of tubulin polymerization. Both compounds were found to be nearly equipotent in the [<sup>3</sup>H]colchicine binding assay. The induction of G2/M arrest was demonstrated for **17b**, being typical for agents that inhibit tubulin polymerization. Notably, no growth inhibitory effect was found in cell-cycle arrested cells (RKOp27). Whereas the effectiveness of numerous clinically anticancer drugs is limited by the fact that they are substrates for the efflux pumps Pgp170 and MRP, **17b** was found to be active toward parental tumor cell lines and multidrug-resistant cell lines. Because of their attractive *in vitro* antitumor profile, we believe that compounds of this structural class are attractive for further structural modifications and that our findings may provide useful information for the design of novel antitumor agents. Investigations on the role of the 10-(2-oxo-2-phenylethylidene)-10H-anthracen-9-ones for antimetabolic activity are in

progress, and results from other modifications will be reported in due course.

## Experimental Section

Melting points were determined with a Kofler melting point apparatus and are uncorrected. Spectra were obtained as follows: <sup>1</sup>H NMR spectra were recorded with a Varian Mercury 400 plus (400 MHz) spectrometer, using tetramethylsilane as an internal standard. Fourier-transform IR spectra were recorded on a Bio-Rad laboratories Typ FTS 135 spectrometer, and analysis was performed with WIN-IR Foundation software. Elemental analyses were performed at the Münster Microanalysis Laboratory, using a Heraeus CHN-O Rapid microanalyzer, and all values were within ±0.4% of the calculated composition. Mass spectra (EI) were recorded in the EI mode using a MAT GCQ Finnigan instrument. For HRMS (ESI-nanospray mode) analysis of **17k**, a LTQ Orbitrap XL (Thermo Fisher Scientific, Bremen) spectrometer was used. All organic solvents were appropriately dried or purified prior to use. Mixtures were stirred magnetically. Solvents were usually removed by rotary evaporation under reduced pressure. α-Keto aldehyde hydrates (phenylglyoxals) were obtained from commercial sources. Analytical TLC used to monitor reactions was done on Merck silica 60 F<sub>254</sub> alumina coated plates (E. Merck, Darmstadt, Germany). Silica gel column chromatography was performed using Acros 60–200 mesh silica gel.

**(10-oxo-10H-Anthracen-9-ylidene) Acetic Acid (14)**. A stirred mixture of 10H-anthracen-9-one **13** (10 g, 51.5 mmol) and glyoxylic acid monohydrate (9.2 g, 100 mmol) in ethanol (150 mL) was heated under reflux (N<sub>2</sub> atmosphere, oil bath, 90 °C). While raising the temperature, a few drops of piperidine were added at such a rate that a clear solution was formed. After 4 h (TLC control, CH<sub>2</sub>Cl<sub>2</sub>), the mixture was cooled to room temperature, poured into H<sub>2</sub>O (400 mL)/6 M HCl (10 mL), and extracted with CH<sub>2</sub>Cl<sub>2</sub> (5 × 50 mL). The combined organic extracts were washed with water and dried over Na<sub>2</sub>SO<sub>4</sub>. Then, the drying agent was removed by filtration and the solvent was evaporated in vacuo to a small volume (30–40 mL). The carboxylic acid crystallized in an ice bath. The crystals were filtered off and washed with cold CH<sub>2</sub>Cl<sub>2</sub> (100 mL) to remove traces of **13** (TLC control, CH<sub>2</sub>Cl<sub>2</sub>). Concentration of the mother liquor gave a small second pale-yellow crop (7.60 g, 59%).

**(10-oxo-10H-Anthracen-9-ylidene) Acetic Acid Methyl Ester (15)**. The carboxylic acid **14** (2.0 g, 7.99 mmol) was added to a solution of methanol (100 mL) and conc H<sub>2</sub>SO<sub>4</sub> (1 mL). The mixture was heated under reflux with stirring for 24 h. After complete conversion (TLC control, CH<sub>2</sub>Cl<sub>2</sub>), the mixture was cooled to room temperature, poured into water (300 mL), and extracted with CH<sub>2</sub>Cl<sub>2</sub> (3 × 50 mL). The combined organic layers were washed with water, dried (Na<sub>2</sub>SO<sub>4</sub>), and concentrated. The residue was then purified by silica gel chromatography (CH<sub>2</sub>Cl<sub>2</sub>) to afford the pure ester as a white solid (1.5 g, 71%). <sup>1</sup>H NMR (CDCl<sub>3</sub>, 400 MHz, 300 K) δ 8.27–8.24 (m, 2H), 7.85–7.80 (m, 2H), 7.66–7.62 (m, 1H), 7.60–7.54 (m, 3H), 6.66 (s, 1H), 3.79 (s, 3H).

**(10-oxo-10H-Anthracen-9-ylidene) Acetyl Chloride (16)**. Thionyl chloride (30 mL) was added to **14** (2.0 g, 7.99 mmol), followed by a catalytic amount of DMF (2 drops). The mixture was heated to reflux for 2 h and then allowed to cool to room temperature. Excess thionyl chloride was removed in vacuo. After treating the residue with *n*-hexane (2 × 30 mL) and evaporation, the crude acid chloride was obtained as a yellow solid (2.0 g, 93%) and used without further purification. <sup>1</sup>H NMR (CDCl<sub>3</sub>, 400 MHz, 300 K) δ 8.26–8.24 (m, 2H), 7.97–7.95 (m, 1H), 7.85–7.83 (m, 1H), 7.69–7.61 (m, 4H), 6.82 (s, 1H).

**10-(2-oxo-2-Phenylethylidene)-10H-anthracen-9-one (17a)**. See Supporting Information for details.

**10-[2-(4-Methoxyphenyl)-2-oxoethylidene]-10H-anthracen-9-one (17b)**. The title compound was prepared from **16** (2.14 g, 8.00 mmol) and methoxybenzene (0.87 mL, 8.00 mmol) in a similar manner as described for the preparation of **17d**.

Purification by silica gel chromatography (CH<sub>2</sub>Cl<sub>2</sub>) afforded **17b** as a pale-yellow powder (0.82 g, 30%); mp 120–122 °C; FTIR

1647 cm<sup>-1</sup>. <sup>1</sup>H NMR (CDCl<sub>3</sub>, 400 MHz, 300 K) δ 8.32 (dd, 1H, *J* = 7.82 Hz, *J* = 1.18 Hz), 8.23 (dd, 1H, *J* = 7.72 Hz, *J* = 1.18 Hz), 7.99 (d, 1H, *J* = 8.41 Hz), 7.85, 6.82 (d, 2H, *J* = 9 Hz), 7.71–7.67 (m, 1H), 7.61–7.56 (m, 2H), 7.43–7.39 (m, 1H), 7.30–7.26 (m, 1H), 7.18 (s, 1H), 3.81 (s, 3H). MS *m/z* 340 (100, M<sup>+</sup>). Anal. (C<sub>23</sub>H<sub>16</sub>O<sub>3</sub>).

**10-[2-(3-Methoxyphenyl)-2-oxoethylidene]-10H-anthracen-9-one (17c)**. 3-Methoxyphenylglyoxal hydrate (0.82 g 5.15 mmol) was added to a solution of **13** (1.00 g, 5.15 mmol) in 50 mL of acetic anhydride, and the mixture was heated to reflux. The solution became orange-red. When the reaction was complete (TLC control, ethyl acetate/petroleum ether 3/7), the mixture was poured into water (100 mL), stirred for 20 min, and then extracted with CH<sub>2</sub>Cl<sub>2</sub> (3 × 50 mL). The combined organic layers were washed with water, dried over Na<sub>2</sub>SO<sub>4</sub>, and the solvent was then evaporated under reduced pressure. The residue was purified by silica gel chromatography (ethyl acetate/petroleum ether 3/7) to afford **17c** as a pale-yellow powder (0.38 g, 22%). <sup>1</sup>H NMR (CDCl<sub>3</sub>, 400 MHz, 300 K) δ 8.32 (dd, 1H, *J* = 7.83 Hz, *J* = 1.17 Hz), 8.23 (dd, 1H, *J* = 7.82 Hz, *J* = 0.78 Hz), 7.99 (d, 1H, *J* = 7.82), 7.72–7.68 (m, 1H), 7.62–7.58 (m, 1H), 7.54 (dd, 1H, *J* = 7.83 Hz, *J* = 0.78 Hz), 7.46–7.40 (m, 3H), 7.31–7.28 (m, 1H), 7.26–7.24 (m, 1H), 7.20 (s, 1H), 7.07–7.04 (m, 1H), 3.78 (s, 3H).

**10-[2-(3,4-Dimethoxyphenyl)-2-oxoethylidene]-10H-anthracen-9-one (17d)**. Anhydrous AlCl<sub>3</sub> (1.07 g, 8.00 mmol) was added in one portion to a suspension of crude **16** (2.14 g, 8 mmol) in DCE (30 mL), and the solution was cooled to 0 °C. After stirring the dark-red solution for 10 min, a solution of 1,2-dimethoxybenzene (1.11 g, 8 mmol) in 5 mL DCE was added dropwise. After stirring for 2 h at 0 °C (TLC control, CH<sub>2</sub>Cl<sub>2</sub>), the reaction mixture was poured into water (300 mL)/6 N HCl (50 mL), stirred for 10 min, and then extracted with CH<sub>2</sub>Cl<sub>2</sub> (4 × 50 mL). The combined organic layers were washed with water, dried (Na<sub>2</sub>SO<sub>4</sub>), and concentrated. Thereafter, the residue was purified by silica gel chromatography (ethyl acetate/petroleum ether 7/3) to afford **17d** as yellow needles (0.97 g, 33%). <sup>1</sup>H NMR (CDCl<sub>3</sub>, 400 MHz, 300 K) δ 8.34–8.32 (m, 1H), 8.25–8.23 (m, 1H), 8.00–7.98 (d, 1H, *J* = 8.00 Hz), 7.72–7.68 (m, 1H), 7.62–7.60 (m, 1H), 7.58–7.55 (m, 1H), 7.50 (d, 1H, *J* = 2.0 Hz), 7.44–7.39 (m, 2H), 7.31–7.27 (m, 1H), 7.17 (s, 1H), 6.71 (d, 1H, *J* = 8.2 Hz), 3.88 (s, 3H), 3.87 (s, 3H).

**10-[2-(3,4-Dihydroxyphenyl)-2-oxoethylidene]-10H-anthracen-9-one (17e)**. 10-[2-(3,4-Dimethoxy-phenyl)-2-oxo-ethylidene]-10H-anthracen-9-one **17d** (0.34 g, 1.00 mmol) was dissolved in CH<sub>2</sub>Cl<sub>2</sub> (10 mL). A solution of boron tribromide (5 mL, 5.00 mmol) in CH<sub>2</sub>Cl<sub>2</sub> (20 mL) was added dropwise with stirring at –78 °C (N<sub>2</sub> atmosphere). Stirring was continued overnight while the mixture was allowed to warm to room temperature. Then the reaction was terminated by addition of water (300 mL), and the product was subsequently extracted with ethyl acetate. The extract was dried with Na<sub>2</sub>SO<sub>4</sub>, and the solvent was then removed in vacuo. The residue was then chromatographed (ethyl acetate/petroleum ether 7/3) to afford a yellow powder (0.10 g, 30%). <sup>1</sup>H NMR (DMSO-*d*<sub>6</sub>, 400 MHz, 300 K) δ 10.01 (s, 1H), 9.43 (s, 1H), 8.26 (d, 1H, *J* = 7.83 Hz), 8.18 (dd, 1H, *J* = 7.83 Hz, *J* = 1.17 Hz), 8.14–8.11 (m, 1H), 7.82–7.78 (m, 1H), 7.68–7.64 (m, 1H), 7.65 (s, 1H), 7.54–7.45 (m, 3H), 7.36–7.34 (m, 2H), 6.77 (d, *J* = 9.00 Hz).

**10-[2-(2,4-Dimethoxyphenyl)-2-oxoethylidene]-10H-anthracen-9-one (17f)**. See Supporting Information for details.

**10-[2-oxo-2-(2,3,4-Trimethoxyphenyl)ethylidene]-10H-anthracen-9-one (17g)**. See Supporting Information for details.

**10-[2-oxo-2-(3,4,5-Trimethoxyphenyl)ethylidene]-10H-anthracen-9-one (17h)**. See Supporting Information for details.

**10-[2-(2-Hydroxy-3,4-dimethoxyphenyl)-2-oxoethylidene]-10H-anthracen-9-one (17i)**. AlCl<sub>3</sub> was added in one portion to a solution of 10-[2,3,4-trimethoxy-phenyl)-2-oxo-ethylidene]-9(10H)-anthracenone (**17h**, 0.40 g, 1.00 mmol) in DCE (25 mL) at 0 °C. When the reaction was completed (TLC control), the mixture was poured into water (400 mL)/6 N HCl (50 mL) and extracted with CH<sub>2</sub>Cl<sub>2</sub> (3 × 30 mL). The combined organic layers were washed with water, dried over Na<sub>2</sub>SO<sub>4</sub>, and the solvent was then evaporated under reduced pressure. The residue was purified by silica gel

chromatography (ethyl acetate/petroleum ether 1:1) to afford **17i** as a pale-yellow powder (0.17 g, 42%). <sup>1</sup>H NMR (CDCl<sub>3</sub>) δ 12.30 (s, 1H), 8.34–8.32 (m, 1H), 8.27–8.24 (m, 1H), 7.98 (d, 1H, *J* = 7.82 Hz), 7.73–7.68 (m, 1H), 7.63–7.59 (m, 1H), 7.49–7.45 (m, 1H); 7.40–7.37 (m, 1H), 7.26 (d, 1H, *J* = 9.00 Hz), 7.14 (s, 1H), 6.30 (d, 1H, *J* = 9.00 Hz), 3.92 (s, 3H), 3.87 (s, 3H).

**10-[2-oxo-2-*p*-tolyl-ethylidene]-10H-anthracen-9-one (17j)**. See Supporting Information for details.

**10-[2-(4-Hydroxy-phenyl)-2-oxo-ethylidene]-10H-anthracen-9-one (17k)**. See Supporting Information for details.

**10-[2-(4-Methoxythiophen-2-yl)-2-oxoethylidene]-10H-anthracen-9-one (17l)**. See Supporting Information for details.

**10-[(2-oxo-2-Thiophen-2-yl-ethylidene)-10H-anthracen-9-one (17m)**. See Supporting Information for details.

**[(10-oxo-(10H)-anthracen-9-ylidene)]-acetic Acid 2-Methoxyphenyl Ester (18a)**. See Supporting Information for details.

**[(10-oxo-(10H)-Anthracen-9-ylidene)]-acetic Acid 2,6-Dimethoxyphenyl Ester (18b)**. See Supporting Information for details.

**10-(1-Hydroxy-2-oxo-2-phenylethyl)-10H-anthracen-9-one (19a)**. A stirred mixture of **13** (1.0 g, 5.15 mmol) and phenylglyoxal hydrate (0.69 g, 5.15 mmol) in ethanol (50 mL) was heated under reflux (N<sub>2</sub> atmosphere, oil bath, 90 °C). While raising the temperature, a few drops of piperidine were added at such a rate that a clear solution was formed. After 4 h (TLC control), the mixture was cooled to room temperature, and the solvent was evaporated in vacuo. Purification of the residue by silica gel chromatography (ethyl acetate/petroleum ether 7/3) afforded **19a** as a pale-yellow powder (0.30 g, 18%); mp 164–165 °C; FTIR 1659 cm<sup>-1</sup>. <sup>1</sup>H NMR (CDCl<sub>3</sub>, 400 MHz, 300 K) δ 8.20–8.18 (m, 1H), 8.07–8.05 (m, 1H), 7.72–7.70 (m, 2H), 7.66–7.65 (m, 1H), 7.62–7.58 (m, 2H), 7.48–7.42 (m, 3H), 7.40–7.36 (m, 1H), 7.23–7.22 (m, 1H), 7.01–6.99 (m, 1H), 5.42 (dd, 1H, *J* = 7.04 Hz, *J* = 2.35 Hz), 4.72 (d, 1H, *J* = 2.34 Hz), 3.54 (d, 1H, *J* = 7.04 Hz). Anal. (C<sub>22</sub>H<sub>16</sub>O<sub>3</sub>).

**10-(1-Hydroxy-2-(4-methoxyphenyl)-2-oxoethyl)-10H-anthracen-9-one (19b)**. See Supporting Information for details.

**10-(1-Hydroxy-2-(3,4,5-trimethoxyphenyl)-2-oxoethyl)-10H-anthracen-9-one (19c)**. See Supporting Information for details.

**2-[(10-Hydroxy-10H-anthracen-9-ylidene)]-1-(4-methoxyphenyl)-ethanone (20)**. Fine powdered sodium borohydride (0.23 g, 6.00 mmol) was added in one portion to a suspension of **17b** (0.34 g, 1 mmol) in a mixture of THF (20 mL) and ethanol (5 mL) at room temperature. When the reaction was completed (TLC control, CH<sub>2</sub>Cl<sub>2</sub>), water (3 mL) was added and the solution was then extracted with CH<sub>2</sub>Cl<sub>2</sub> (50 mL). The extract was dried with Na<sub>2</sub>SO<sub>4</sub>, and the solvent was then removed in vacuo. The residue was chromatographed on a column of SiO<sub>2</sub> (ethyl acetate/petroleum ether 7/3) to afford **20** as a yellow powder (98 mg, 29%); mp 170 °C; FTIR 3421, 1638, cm<sup>-1</sup>. <sup>1</sup>H NMR (CDCl<sub>3</sub>, 400 MHz, 300 K) δ 7.95, 6.84 (d, 2H, *J* = 5.08 Hz), 7.81–7.79 (m, 1H), 7.72–7.70 (m, 1H), 7.62 (d, 1H, *J* = 7.44 Hz), 7.45–7.41 (m, 3H), 7.29–7.26 (m, 1H), 7.09–7.05 (m, 1H), 6.95 (s, 1H), 5.66 (s, 1H), 3.82 (s, 3H). MS *m/z* 342 (14.49, M<sup>+</sup>), 325 (100). Anal. (C<sub>23</sub>H<sub>18</sub>O<sub>3</sub>).

**2-(Anthracen-9-yloxy)-1-(4-methoxyphenyl)-ethanone (22)**. 9-(10H)-Anthracenone (**13**, 1 g, 5.15 mmol) and dry K<sub>2</sub>CO<sub>3</sub> (7.00 g, 50.75 mmol) were suspended in absolute acetone (50 mL) under N<sub>2</sub>. 2-Bromo-4'-methoxyacetophenone (1.19 g, 5.2 mmol) was added, and the mixture was refluxed under nitrogen until the reaction was completed (TLC control, CH<sub>2</sub>Cl<sub>2</sub>). The reaction mixture was then cooled and poured into water (400 mL), acidified with 6 N HCl, and extracted with CH<sub>2</sub>Cl<sub>2</sub> (3 × 30 mL). The combined CH<sub>2</sub>Cl<sub>2</sub> extracts were washed, dried over Na<sub>2</sub>SO<sub>4</sub>, and then evaporated. Purification by silica gel chromatography (CH<sub>2</sub>Cl<sub>2</sub>/hexane 8/2) afforded **22** as a pale-yellow powder (0.25 g, 14%). <sup>1</sup>H NMR (CDCl<sub>3</sub>, 400 MHz, 300 K) δ 8.35–8.33 (s, 2H), 8.28 (s, 1H), 8.03–8.00 (s, 2H), 7.96 (d, 2H, *J* = 9.0 Hz), 7.49–7.47 (m, 4H), 6.95 (d, 2H, *J* = 9.0 Hz), 5.48 (s, 2H), 3.87 (s, 3H);

**10-(1-Hydroxy-2,2-dimethoxy-ethyl)-10H-anthracen-9-one (23)**. See Supporting Information for details.

**Biological Assay Methods. Cells and Culture Conditions.** Human chronic myelogenous K562 leukemia cells were obtained from DSMZ, Braunschweig, Germany, and cultured in RPMI 1640

medium (Gibco) containing 10% fetal bovine serum (FBS, Biobrom KG), streptomycin (0.1 mg/mL), penicillin G (100 units/mL), and L-glutamine (30 mg/L) at 37 °C in 5% CO<sub>2</sub>. Cell line SF268 (central neural system carcinoma) were obtained from NCI. The human tumor cell lines KB/HeLa (cervical carcinoma), SKOV3 (ovarian adenocarcinoma), NCI-H460, and L1210 (murine leukemia) were obtained from ATCC. The RKO human colon adenocarcinoma cells containing an ecdysone-inducible expression vector of p27<sup>Kip1</sup> were described recently.<sup>43</sup> The L1210<sup>VCR</sup> cell line (expression of MDR-1, MRP-1 negative) was described recently.<sup>44</sup> Rat LT12 cells, the LT12/MDR subline (ectopic expression of human MDR-1 protein) as well as P388 cells and the P388/Adr subline (selected with doxorubicine, elevated levels of MDR-1 protein) were provided by Dr. Nooter (University Hospital, Rotterdam, The Netherlands).

**Assay of Cell Growth.** First, K562 cells were plated at 2 × 10<sup>5</sup> cells/mL in 48 well dishes (Costar, Cambridge, MA). Then untreated control wells were assigned a value of 100%. Drugs were made soluble in DMSO/methanol 1:1, and control wells received equal volumes (0.5%) of vehicle alone. Drugs were dissolved in methanol/DMSO 1:1. To each well were added 5 μL of drug and the final volume in the well was 500 μL. Cell numbers were counted with a Neubauer counting chamber (improved, double grid) after treatment with chemicals for 48 h. Each assay condition was prepared in triplicate, and the experiments were carried out three times. IC<sub>50</sub> values were obtained by nonlinear regression (GraphPad Prism) and represent the concentration at which cell growth was inhibited by 50%. The adjusted cell number was calculated as a percentage of the control, which was the number of cells in wells without the addition of compound.

**XTT Assay.** The XTT assay was used to determine proliferation by quantification of cellular metabolic activity.<sup>29</sup> IC<sub>50</sub> values were obtained by nonlinear regression (GraphPad Prism). The various tumor cell lines were seeded in microtiter plates in a density of 1 × 10<sup>3</sup>–8 × 10<sup>4</sup> cells/well in 125 μL for logarithmic cell growth and were incubated with different concentrations of cytotoxic agents for 48 h.

In RKO p27<sup>Kip1</sup> cells, expression of p27<sup>Kip1</sup> was induced by 3 μM ponasterone A in 24 h, leading to an arrest of these cells in the G1 phase of the division cycle. Cell cycle specific substances, such as tubulin inhibitors, were only cytotoxic if the cells were not arrested and the cell cycle was in progress. The assay was performed in 96-well plates. The cell count of induced cells was about three times higher than that of noninduced cells. RKO cells with/without p27<sup>Kip1</sup> expression (2 × 10<sup>4</sup> cells/well induced; 6 × 10<sup>3</sup> cells/well not induced, in 125 μL) were treated with the test compound for 48 h at 37 °C. The controls were untreated cells (± induction). On day 1, the cells were plated (± ponasterone A) and incubated at 37 °C for 24 h. On day 2, the test substance was added (control DMSO) and incubation at 37 °C was continued for another 48 h. Thereafter, a standard XTT assay was carried out.

**Flow Cytometric Analysis of Cell-Cycle Status.** For a concentration-dependent cell cycle analysis, subconfluent KB/HeLa cells were exposed to test compounds for 24 h at 37 °C, detached, and collected. After fixation with 70% ethanol, the DNA was simultaneously stained by propidium iodide and digested with RNase. The DNA content of cells was determined with a FACS Calibur™ cytometer (Beckton Dickinson, Heidelberg, Germany). The number of cells in G2/M phase was calculated by cell cycle analysis software (Mod Fit LT; VERITY). IC<sub>50</sub> values were calculated by nonlinear regression (GraphPad Prism).

**Isolation of MTP and In Vitro MT Assembly Assay by Turbidimetric Measurement.** Microtubule protein (MTP) consisting of 80–90% tubulin and 10–20% microtubule associated proteins (MAPs) was isolated from porcine brain by two cycles of temperature-dependent disassembly (0 °C)/reassembly (37 °C) according to the method described by Shelanski et al.<sup>45</sup> Throughout the preparation, a buffer containing 20 mM PIPES (1,4-piperazine diethane sulfonic acid, pH 6.8), 80 mM NaCl, 0.5 mM MgCl<sub>2</sub>, 1 mM EGTA (ethylene bis(oxyethylenitrilo) tetraacetic acid), and 1 mM DTT was used. To increase the yield,

the reassembly steps were performed in the presence of glycerol.<sup>46</sup> The protein concentration was determined by the Lowry procedure using bovine serum albumin as a standard. Satisfactory purity of the MTP was reached after the second cycle of assembly and disassembly. Microtubules to be used for determining antimicrotubule effector activities were prepared by in vitro self-assembly of MTP in presence of GTP (guanosin-5'-triphosphate) and magnesium ions. The MTP concentration for assembly was 1.2 mg/mL (determined by the Lowry procedure using bovine serum albumin as a standard). The assembly measurements were done directly in cuvettes. To start microtubule formation, the stock MTP solutions were diluted with the preparation buffer to 1.2 mg/mL, GTP was added to 0.6 mM (final concentration), and the samples were transferred into spectrophotometer (Cary 4E, Varian Inc.), equipped with a temperature-controlled multichannel cuvette holder, adjusted to 37 °C. Turbidity was recorded over 30 min at 360 nm.

The tubulin effectors were added from stock solutions in DMSO. The final DMSO concentration was 1%. Control measurements were made with DMSO, only. To quantify the drug activity, the turbidity signal after 30 min (plateau level, representing the assembly/disassembly steady state) was compared with that of the control samples. The IC<sub>50</sub> value is defined as the drug concentration that causes a 50% inhibition in relation to the assembly level without the drug.

**<sup>3</sup>H Colchicine Competition-Binding Assay.**<sup>37</sup> <sup>3</sup>H-Colchicine was diluted and biotin-labeled tubulin (T333, Cytoskeleton, Denver, CO) was reconstituted according to the manufacturers protocol. The diluted compounds and the <sup>3</sup>H-colchicine were transferred to a 96-well isoplate (PE-Wallac, Boston, MA), and buffer and the reconstituted biotin-labeled tubulin were added. After incubation, streptavidin-coated yttrium SPA beads (Amersham Pharmacia Biotech, Piscataway, NJ) were added and the bound radioactivity was determined using a MicroBeta Trilux Microplate scintillation counter (PE-Wallac Boston, MA). IC<sub>50</sub> values were obtained by nonlinear regression (GraphPad Prism).

**Acknowledgment.** We thank Cornelia Lang, Britta Kroenert, Sonja Seidel, Katrin Zimmermann, Magnus Bröcker, Marcel Overmann, and Angelika Zinner for excellent technical assistance.

**Supporting Information Available:** IR, <sup>1</sup>H NMR, and MS data of new compounds **17a–17m**, **18a–18b**, **19a–19c**, **20**, **22**, and **23**, cell cycle analysis data of KB/HeLa cells treated with **17b** and reference compounds, table of elemental analysis results of all target compounds. This material is available free of charge via the Internet at <http://pubs.acs.org>.

## References

- Honore, S.; Pasquier, E.; Braguer, D. Understanding microtubule dynamics for improved cancer therapy. *Cell. Mol. Life Sci.* **2005**, *62*, 3039–3056.
- Pellegrini, F.; Budman, D. R. Review: tubulin function, action of antitubulin drugs, and new drug development. *Cancer Invest.* **2005**, *23*, 264–273.
- Hearn, B. R.; Shaw, S. J.; Myles, D. C. Microtubule targeting agents. *Compr. Med. Chem. II* **2007**, *7*, 81–110.
- Jordan, M. A. Mechanism of action of antitumor drugs that interact with microtubules and tubulin. *Curr. Med. Chem. Anticancer Agents* **2002**, *2*, 1–17.
- Li, Q.; Sham, H. L. Discovery and development of antimetabolic agents that inhibit tubulin polymerisation for the treatment of cancer. *Expert Opin. Ther. Patents* **2002**, *12*, 1663–1702.
- Mahindroo, N.; Liou, J. P.; Chang, J. Y.; Hsieh, H. P. Antitubulin agents for the treatment of cancer—a medicinal chemistry update. *Expert Opin. Ther. Patents* **2006**, *16*, 647–691.
- Pettit, G. R.; Singh, S. B.; Hamel, E.; Lin, C. M.; Alberts, D. S.; Garcia-Kendall, D. Isolation and structure of the strong cell growth and tubulin inhibitor combretastatin A-4. *Experientia* **1989**, *45*, 209–211.
- Goodin, S.; Kane, M. P.; Rubin, E. H. Epothilones: mechanism of action and biologic activity. *J. Clin. Oncol.* **2004**, *22*, 2015–2025.
- Yoshimatsu, K.; Yamaguchi, A.; Yoshino, H.; Koyanagi, N.; Kitoh, K. Mechanism of action of E7010, an orally active sulfonamide antitumor agent: inhibition of mitosis by binding to the colchicine site of tubulin. *Cancer. Res.* **1997**, *57*, 3208–3213.
- Sirisoma, N.; Kasibhatla, S.; Pervin, A.; Zhang, H.; Jiang, S.; Willardsen, J. A.; Anderson, M. B.; Baichwal, V.; Mather, G. G.; Jessing, K.; Hussain, R.; Hoang, K.; Pleiman, C. M.; Tseng, B.; Drewe, J.; Cai, S. X. Discovery of 2-chloro-N-(4-methoxyphenyl)-N-methylquinazolin-4-amine (EPI28265, MPI-0441138) as a potent inducer of apoptosis with high in vivo activity. *J. Med. Chem.* **2008**, *51*, 4771–4779.
- Baasner, S.; Emig, P.; Gerlach, M.; Müller, G.; Paulini, K.; Schmidt, P.; Burger, A. M.; Fiebig, H.-H.; Günther, E. G. D-82318—A novel, synthetic, low molecular weight tubulin inhibitor with potent in vivo antitumor activity. EORTC-NCI-AACR Meeting, Frankfurt, Germany, 2002, Poster 112.
- Meng, F.; Cai, X.; Duan, J.; Matteucci, M. G.; Hart, C. P. A novel class of tubulin inhibitors that exhibit potent antiproliferation and in vitro vessel-disrupting activity. *Cancer Chemother. Pharmacol.* **2008**, *61*, 953–963.
- Zhang, L. H.; Wu, L.; Raymon, H. K.; Chen, R. S.; Corral, L.; Shirley, M. A.; Narla, R. K.; Gamez, J.; Muller, G. W.; Stirling, D. I.; Bartlett, J. B.; Schafer, P. H.; Payvandi, F. The synthetic compound CC-5079 is a potent inhibitor of tubulin polymerization and tumor necrosis factor- $\alpha$  production with antitumor activity. *Cancer. Res.* **2006**, *66*, 951–959.
- Hadfield, J. A.; Ducki, S.; Hirst, N.; McGown, A. T. Tubulin and microtubules as targets for anticancer drugs. *Prog. Cell Cycle Res.* **2003**, *5*, 309–25.
- Prinz, H.; Ishii, Y.; Hirano, T.; Stoiber, T.; Camacho Gomez, J. A.; Schmidt, P.; Düssmann, H.; Burger, A. M.; Prehn, J. H.; Günther, E. G.; Unger, E.; Umezawa, K. Novel benzylidene-9(10H)-anthracenones as highly active antimicrotubule agents. Synthesis, antiproliferative activity, and inhibition of tubulin polymerization. *J. Med. Chem.* **2003**, *46*, 3382–3394.
- Zuse, A.; Schmidt, P.; Baasner, S.; Böhm, K. J.; Müller, K.; Gerlach, M.; Günther, E. G.; Unger, E.; Prinz, H. 9-Benzylidene-naphtho[2,3-b]thiophen-4-ones as novel antimicrotubule agents—synthesis, antiproliferative activity, and inhibition of tubulin polymerization. *J. Med. Chem.* **2006**, *49*, 7816–7825.
- Zuse, A.; Schmidt, P.; Baasner, S.; Böhm, K. J.; Müller, K.; Gerlach, M.; Günther, E. G.; Unger, E.; Prinz, H. Sulfonate derivatives of naphtho[2,3-b]thiophen-4(9H)-one and 9(10H)-anthracenone as highly active antimicrotubule agents. Synthesis, antiproliferative activity, and inhibition of tubulin polymerization. *J. Med. Chem.* **2007**, *50*, 6059–6066.
- Lawrence, N. J.; McGown, A. T. The chemistry and biology of antimetabolic chalcones and related enone systems. *Curr. Pharm. Des.* **2005**, *11*, 1679–1693.
- Liou, J. P.; Chang, J. Y.; Chang, C. W.; Chang, C. Y.; Mahindroo, N.; Kuo, F. M.; Hsieh, H. P. Synthesis and structure–activity relationships of 3-aminobenzophenones as antimetabolic agents. *J. Med. Chem.* **2004**, *47*, 2897–2905.
- Afsah, E. M.; Etman, H. A.; Hamama, W. S.; Sayed-Ahmed, A. F. A study on the reaction of 1,3-indandione with Schiff bases: synthesis of new 1,3-indandiones with expected psychopharmacological and anticoagulant activity. *Boll. Chim. Farm.* **1998**, *137*, 244–248.
- El-Sha'fe, S. M. M. Synthesis of 10-arylidene-9-anthrones and related compounds. *Indian J. Chem.* **1978**, *16B*, 828–830.
- Bergmann, E. D.; Rabinovitz, M.; Gily, S. A ring enlargement in the 9,10-dihydroanthracene series. *Tetrahedron Suppl.* **1966**, *8*, 141–148.
- Weitz, E. Über einige Anthronabkömmlinge. *Liebigs Ann. Chem.* **1919**, *418*, 29–35.
- Rappoport, Z.; Apeloig, Y.; Greenblatt, J. Vinylic cations from solvolysis. 29. Solvolysis of 9-( $\alpha$ -bromoarylidene)anthrones as a probe to the reactivity–selectivity relationship in solvolysis reactions. *J. Am. Chem. Soc.* **1980**, *102*, 3837–3848.
- Müller, K.; Gürster, D.; Piwek, S.; Wiegrebe, W. Antipsoriatic anthrones with modulated redox properties. 1. Novel 10-substituted 1,8-dihydroxy-9(10H)-anthracenones as inhibitors of 5-lipoxygenase. *J. Med. Chem.* **1993**, *36*, 4099–4107.
- Baba, H.; Takemura, T. Spectrophotometric investigations of the tautomeric reaction between anthrone and anthranol. I. The keto-enol equilibrium. *Tetrahedron* **1968**, *24*, 4779–4791.
- Martin, R. Études sur la réaction de fries. XIV. Mécanismes engendrés dans les réactions acido-catalysées. IV. Préparation des acyl-5 gaiacols. *Bull. Soc. Chim. Fr.* **1977**, 901–905.
- Lozzio, C. B.; Lozzio, B. B. Human chronic myelogenous leukemia cell-line with positive philadelphia chromosome. *Blood* **1975**, *45*, 321–334.
- Scudiero, D. A.; Shoemaker, R. H.; Paull, K. D.; Monks, A.; Tierney, S.; Nofziger, T. H.; Currens, M. J.; Seniff, D.; Boyd, M. R. Evaluation of a soluble tetrazolium/formazane assay for cell growth and drug

- sensitivity in culture using human and other tumor cell lines. *Cancer Res.* **1988**, *48*, 4827–4833.
- (30) Schmidt, M.; Lu, Y.; Parant, J. M.; Lozano, G.; Bacher, G.; Beckers, T.; Fan, Z. Differential roles of p21<sup>Waf1</sup> and p27<sup>Kip1</sup> in modulating chemosensitivity and their possible application in drug discovery studies. *Mol. Pharmacol.* **2001**, *60*, 900–906.
- (31) Dumontet, C.; Jaffrezou, J. P.; Tsuchiya, E.; Duran, G. E.; Chen, G.; Derry, W. B.; Wilson, L.; Jordan, M. A.; Sikic, B. I. Resistance to microtubule-targeted cytotoxins in a K562 leukemia cell variant associated with altered tubulin expression and polymerization. *Bull. Cancer* **2004**, *91*, 81–112.
- (32) Dumontet, C.; Sikic, B. I. Mechanism of action of and resistance to antitubulin agents: microtubule dynamics, drug transport, and cell death. *J. Clin. Oncol.* **1999**, *3*, 1061–1070.
- (33) Fardel, O.; Lecreur, V.; Guillouzo, A. The P-glycoprotein multidrug transporter. *Gen. Pharmacol.* **1996**, *27*, 1283–1291.
- (34) Cole, S. P.; Deeley, R. G. Multidrug resistance mediated by the ATP-binding cassette transporter protein MRP. *BioEssays* **1998**, *20*, 931–940.
- (35) Kavallaris, M.; Annereau, J. P.; Barret, J. M. Potential mechanisms of resistance to microtubule inhibitors. *Semin. Oncol.* **2008**, *35*, 22–27.
- (36) Verrills, N. M.; Kavallaris, M. Improving the targeting of tubulin-binding agents: lessons from drug resistance studies. *Curr. Pharm. Des.* **2005**, *11*, 1719–1733.
- (37) Tahir, S. K.; Kovar, P.; Rosenberg, S.; Ng, S.-C. A rapid colchicine competition-binding scintillation proximity assay using biotin-labeled colchicine. *Biotechniques* **2000**, *29*, 156–160.
- (38) Bai, R.; Roach, M. C.; Jayaram, S. K.; Barkoczy, J.; Pettit, G. R.; Luduena, R. F.; Hamel, E. Differential effects of active isomers, segments, and analogs of dolastatin 10 on ligand interactions with tubulin. Correlation with cytotoxicity. *Biochem. Pharmacol.* **1993**, *45*, 1503–1515.
- (39) Bai, R. L.; Pettit, G. R.; Hamel, E. Binding of dolastatin 10 to tubulin at a distinct site for peptide antimetabolic agents near the exchangeable nucleotide and vinca alkaloid sites. *J. Biol. Chem.* **1990**, *265*, 17141–17149.
- (40) Ravelli, R. B.; Gigant, B.; Curmi, P. A.; Jourdain, I.; Lachkar, S.; Sobel, A.; Knossow, M. Insight into tubulin regulation from a complex with colchicine and a stathmin-like domain. *Nature* **2004**, *428*, 198–202.
- (41) Nguyen, T. L.; McGrath, C.; Hermone, A. R.; Burnett, J. C.; Zaharevitz, D. W.; Day, B. W.; Wipf, P.; Hamel, E.; Gussio, R. A common pharmacophore for a diverse set of colchicine site inhibitors using a structure-based approach. *J. Med. Chem.* **2005**, *48*, 6107–6116.
- (42) Zefirova, O. N.; Diikov, A. G.; Zyk, N. V.; Zefirov, N. S. Ligands of the colchicine site of tubulin: a common pharmacophore and new structural classes. *Russ. Chem. Bull. Int. Ed.* **2007**, *56*, 680–688.
- (43) Schmidt, M.; Lu, Y.; Liu, B.; Fang, M.; Mendelsohn, J.; Fan, Z. Differential modulation of paclitaxel-mediated apoptosis by p21<sup>waf1</sup> and p27<sup>kip1</sup>. *Oncogene* **2000**, *19*, 2423–2429.
- (44) Bacher, G.; Nickel, B.; Emig, P.; Vanhoefer, U.; Seeber, S.; Shandra, A.; Klenner, T.; Beckers, T. D-24851, a novel synthetic microtubule inhibitor, exerts curative antitumoral activity in vivo, shows efficacy toward multidrug-resistant tumor cells, and lacks neurotoxicity. *Cancer Res.* **2001**, *61*, 392–399.
- (45) Shelanski, M. L.; Gaskin, F.; Cantor, C. R. Microtubule assembly in the absence of added nucleotides. *Proc. Nat. Acad. Sci. U.S.A.* **1973**, *70*, 765–768.
- (46) Vater, W.; Böhm, K. J.; Unger, E. A simple method to obtain brain microtubule protein poor in microtubule-associated proteins. *Acta Histochem. Suppl.* **1986**, *33*, 123–129.

JM801338R